On the long-time behavior of unsplit Perfectly Matched Layers

Eliane Bécache,* Peter G. Petropoulos† and Stephen D. Gedney ‡

Abstract

We show how to eliminate an undesirable long-time linear growth [11] of the electromagnetic field in a class of unsplit Perfectly Matched Layers (PML) typically used as Absorbing Boundary Conditions in Computational Electromagnetics codes. For the new PML equations we give energy arguments that show the fields in the layer are bounded by a time-independent constant hence they are long-time stable. Numerical experiments confirm the elimination of the linear growth, and the long-time boundedness of the fields.

1 Introduction

The introduction by Bérenger [1] of the concept of the (split) Perfectly Matched Layer as an Absorbing Boundary Condition (ABC) has resulted in much work towards eliminating as an issue the presence of an artificial outer boundary in numerical simulations of wave problems embedded in an infinite background. There are now two related versions of the PML, split [1] and unsplit [2]-[3]. In addition to the application it finds in Computational Electromagnetics, the PML idea has also been applied to wave problems in acoustics [4, 5], elasticity [6], and shallow water waves [7].

Initially it was thought that perturbations of the weakly well-posed split PML [8] give rise to exponentially growing solutions (genuine instability); this has encouraged efforts to develop the unsplit PML [2]-[3], where the layer equations arise from a zero-order perturbation of the Maxwell operator so that strong well-posedness is maintained, as was shown in [9]-[10]. Subsequently, Abarbanel *et. al.* [11] have provided an analysis that explains an observed late-time linear growth of the amplitude of the axial field in the standard unsplit two-dimensional PML in rectangular coordinates. Late time in the context of [11] means "long after the pulse has passed through the PML, i.e., the solution is essentially constant in space." The equations they label as those representing a "physical PML" will be referred to herein as the standard unsplit PML (also see the Appendix and Equation (2.4) of [10]). Further, [11] offers a remedy which, while removing the observed linear growth as verified with numerical experiments employing the "physical PML," nevertheless results in the loss of the perfectly matched property of the air/PML interface. Recently, Bécache & Joly [12] showed that the split PML has at worst a linearly growing solution in the late-time, i.e., not a genuine instability, and related these equations to those of the unsplit version as presented in [2].The possibility of existence of such a linear growth was shown in [12] via Fourier analysis and energy estimates for both the split and the unsplit PML (their unsplit equations are related to those of the "physical" PML considered in [11]). We briefly review in Section 2 these theoretical results, and add a new one regarding the energy in the corner unsplit PML (where two layers meet to enclose a rectangular domain). In [13], an analysis, based on a technical mistake regarding the Kramers-Kronig relations in a conducting medium, erroneously

showed that the standard split/unsplit PML is not causal and an alternative scaling function was proposed as necessary in order to restore causality. Later, [14]-[15] described time-domain implementations of the unsplit PML employing this alternative scaling function, labeled it the "Complex Frequency Shifted" scaling function (hereafter referred to as "the CFS"), and showed that its use is beneficial for simulations in elongated domains. One of the present authors has also briefly considered in [10] the possible benefit of employing the CFS in the unsplit PML for the three common coordinate systems. Briefly, it was found that the CFS results in the correct zero-frequency limit for the unsplit PML, i.e., it reduces the relevant equations to Laplace's equation with the coordinate into the PML appropriately stretched. Thus, using the CFS, the resulting PML equations correctly account for any DC component in the simulation space that reaches the layer where they are imposed. In [10] it was shown that the standard time-domain unsplit PML is governed by a causal (and symmetric) hyperbolic system independently of the choice of the scaling function as long as the high-frequency limit ($\omega \to \infty$) of the scaling function is a real constant.

In the present paper we determine that the CFS removes the late-time linear growth of the axial fields discussed in [11] for the standard two-dimensional unsplit PML and, at the same time, preserves both the perfectly matched property of the layer and the symmetric hyperbolic character (which results in strong well-posedness) of the resulting PML equations in the time-domain. This is accomplished in Section 3 by simply changing the fundamental scaling function (Equation (2.4), [10]) used to derive unsplit PML's in rectangular, cylindrical and spherical coordinates to the CFS scaling function (Equation (9) below). Consequently, the CFS remedy can also be applied to the three-dimensional unsplit PML in all separable coordinate systems of interest to Computational Electromagnetics. In Section 4 we derive the equivalent of (2)-(3) and (5), given below, for the resulting new unsplit PML and show that now all fields are controlled by a constant, i.e., the linear growth of the standard unsplit PML is not allowed. Section 5 presents numerical experiments that validate our analysis. The paper concludes in Section 6 with a short summary.

Notations. We denote by $(.,.)$ the L^2 scalar product in $\mathbb{R}^2$ and by $\|.\|$ the associated norm.

2 Long-time behavior of the standard unsplit PML: A review

We first review some theoretical results applicable to the standard unsplit PML. Also, we present a new result regarding the decay of the zero-order field energy in a corner unsplit PML (i.e., the region where two layers meet in order to completely surround a rectangular computational domain).

Bécache & Joly [12] analyzed the 2D unsplit PML oriented in the direction parallel to the $\hat{y}$−direction in the TE polarization for the fields $\mathbf{E} = (E_x, E_y, 0)^T$ and $\mathbf{H} = (0, 0, H_z)^T$. We review those results after translating them to the polarization and layer orientation considered in our Section 3, i.e., by considering an absorbing layer in the $\hat{z}$−direction (lying parallel to the $\hat{x}$−direction). The relevant PML equations are:

$$\partial_t E_y + \sigma E_y = \partial_z H_x - \partial_x H_z$$

$$\partial_t H_x + \sigma H_x = \partial_z E_y$$

$$\partial_t H_z^\star = -\partial_x E_x \tag{1}$$

$$\partial_t H_z^\star + \sigma H_z^\star = \partial_t H_z,$$

where σ is a positive function of z. The following identity (equivalent to Lemma 2.2, [12]) is satisfied by a first-order energy of (1):

$$\frac{d}{dt}\mathcal{E}_1(t) = -2\sigma \|\partial_t H_x\|_{L^2}^2 \leq 0, \tag{2}$$

where
$$\mathcal{E}_1(t) = \frac{1}{2}(||\partial_t H_z||_{L^2}^2 + ||\partial_t H_x||_{L^2}^2 + ||\sigma H_x||_{L^2}^2 + ||\partial_t E_y + \sigma E_y||_{L^2}^2), \tag{3}$$

with σ being a positive constant. Equations (2)-(3) indicate that the quantities $\partial_t E_y + \sigma E_y$, H_x, and $\partial_t H_z$ are bounded by a time-independent constant; therefore, H_z can grow as $\sim t$, while H_x and E_y (see Lemma 2 in Section 4.1 below) are bounded by time-independent constants.

For the corner PML (where the $\hat{x}$−directed layer overlaps the $\hat{z}$−directed layer), and for $\sigma_x(x) = \sigma_z(z) = \sigma$ constant, the governing equations are (see [9]-[10]):

$$\partial_t E_y + 2\sigma E_y + \sigma^2 \int_0^t E_y(t^{'})dt^{'} = \partial_z H_x - \partial_x H_z \quad (a)$$

$$\partial_t H_x = \partial_z E_y \qquad\qquad (b) \tag{4}$$

$$\partial_t H_z = -\partial_x E_y \qquad\qquad (c).$$

Theorem 1 *The solution of (4) satisfies the following estimate, $\exists\, C > 0$ independent of t such that*

$$\mathcal{E}_0(t) = \frac{1}{2}(||E_y||^2 + ||H_x||^2 + ||H_z||^2) \leq C. \tag{5}$$

Proof: Multiply (4)-(a) with E_y, (4)-(b) with H_x and (4)-(c) with H_z, integrate over all of $\mathbb{R}^2$, and add to obtain, using integration by parts,

$$\frac{d}{dt}\mathcal{E}_0(t) + \sigma^2 (E_y(t), \int_0^t E_y(t^{'})dt^{'}) = -2\sigma||E_y||^2. \tag{6}$$

Let $F(t) = \int_0^t E_y(t^{'})dt^{'}$, so $(E_y(t), \int_0^t E_y(t^{'})dt^{'}) = (\frac{dF(t)}{dt}, F(t)) = \frac{1}{2}\frac{d}{dt}||F(t)||^2$. Then (6) becomes

$$\frac{d}{dt}(\mathcal{E}_0(t) + \frac{\sigma^2}{2}||F(t)||^2) = -2\sigma||E_y||^2. \tag{7}$$

The proof concludes by noting that (7) implies $\mathcal{E}_0(t) + \frac{\sigma^2}{2}||F(t)||^2 \leq constant\ \forall t$. ∎

It should be emphasized that [12] rigorously shows that the electromagnetic PML derived from Maxwell's equations does not possess exponentially growing solutions, i.e., no genuine instabilities, hence the source of exponential instabilities of the type described in [16] must be sought elsewhere.

Before proceeding it is instructive to consider the Helmholtz equation satisfied by the electric field, $E_y(x, z, \omega)$, in the standard unsplit PML. Following [10] we have:

$$\partial_x^2 E_y + \frac{1}{\alpha_z(z, \omega)}\partial_z(\frac{1}{\alpha_z(z, \omega)}\partial_z E_y) + \omega^2\varepsilon\mu E_y = 0, \tag{8}$$

where $\alpha_z(z, \omega) = \xi_z(1 + \frac{\sigma_z(z)}{-i\omega})$. The $\omega \to 0$ limit of (8), which corresponds to $t \to \infty$ in the time-domain, does not result in Laplace's equation for E_y; one obtains $\partial_x^2 E_y = 0$ instead. Consequently, the standard unsplit PML cannot be expected to absorb evanescent waves, or to behave properly in long-time simulations.

Even though the standard unsplit PML layer suffers in the long time as described above, this suffering cannot affect the solution in the interior computational domain due to the way electromagnetic waves transport energy. Since, as shown above for the polarization considered herein, the fields E_y and H_x remain bounded (they actually decay to zero in computations) no energy can exit normally from the PML towards the interior computational domain. Also, the energy (which goes like t^2) transported along the layer due to E_y and H_z cannot manifest itself

3

inside the computational domain since during actual computations in rectangular coordinates this energy will enter the corner layer and will be absorbed. Of course this requires the numerical scheme to satisfy a discrete analog of the Poynting theorem. This is the case for the Yee scheme [19] employed in our Section 5; the contamination of the interior computational domain shown in [11] may possibly be traced to the numerical scheme employed therein not possessing a discrete Poynting theorem. Also, for other wave propagation problems, e.g., elasticity, it may be possible that the linear growth of some field components inside the PML will eventually contaminate the interior computational domain irrespective of the numerical scheme employed.

3 CFS unsplit PML model equations

In our analysis we will consider a Transverse Magnetic polarization electromagnetic problem on the plane $(x, z) \in (-\infty, \infty) \times [-\infty, d]$ for the fields $\mathbf{E} = (0, E_y, 0)^T$ and $\mathbf{H} = (H_x, 0, H_z)^T$, and a PML that occupies the region $(x, z) \in (-\infty, \infty) \times [0, d]$ where d is the width of the PML. The medium permittivity is ε, and the permeability is μ. We proceed according to [10] choosing, instead of Equation (2.4) in that paper,

$$\alpha_z(z, \omega) = \xi_z(1 + \frac{\sigma_z(z)}{\gamma - i\omega}), \tag{9}$$

where the role of ξ_z is explained in [10], $\sigma_z(z)$ is a positive function (not necessarily zero at $z = 0$) typically defined as $\sigma_z(z) = \sigma_{max}(\frac{z}{d})^m$ where m is an integer, and $\gamma \geq 0$ is a new parameter.

Particularizing Equation (A.3) of [10] to the geometry given above, the following frequency-domain Maxwell system in the PML region is obtained (employing an $e^{-i\omega t}$ time convention):

$$-i\omega D_y = \partial_z H_x - \partial_x H_z$$

$$D_y = \xi_z \varepsilon (1 + \frac{\sigma_z(z)}{\gamma - i\omega}) E_y$$

$$-i\omega B_x = \partial_z E_y$$

$$B_x = \xi_z \mu (1 + \frac{\sigma_z(z)}{\gamma - i\omega}) H_x \tag{10}$$

$$-i\omega B_z = -\partial_x E_y$$

$$B_z = \frac{\mu}{\xi_z} (\frac{\gamma - i\omega}{\sigma_z(z) + \gamma - i\omega}) H_z.$$

System (10), in contrast to the standard unsplit PML, gives the correct $\omega \to 0$ limit as we now show. Using (9) in (8), one finds that, for $\omega \to 0$, the electric field E_y satisfies

$$\partial_x^2 E_y + \frac{1}{\xi_z(1 + \frac{\sigma_z(z)}{\gamma})} \partial_z \left(\frac{1}{\xi_z(1 + \frac{\sigma_z(z)}{\gamma})} \partial_z E_y \right) = 0, \tag{11}$$

i.e., it satisfies Laplace's equation with the coordinate into the PML stretched as $z' = z_0 + \int_{z_0}^{z} \xi_z(1 + \frac{\sigma_z(s)}{\gamma}) ds$. This is the source of the superior performance over the standard unsplit PML illustrated in [15] for elongated domains and in [17] for evanescent waves in waveguides. Also, the presence of γ results in the loss of the property of frequency-independent damping evident in the standard unsplit PML. The magnitude of the reflection coefficient for a plane wave incident on the layer modeled by (10), and terminated with a Dirichlet boundary condition, now is

$$|R| = e^{-2\sqrt{\varepsilon\mu}\kappa_z \xi_z \frac{\omega^2}{\gamma^2 + \omega^2} \int_0^z \sigma(s) ds}, \tag{12}$$

4

where κ_z is the $\hat{z}$-component of the incident wave vector. In practice, the frequency variation in (12) is not detrimental as we now explain ; picking γ to be the lowest frequency contributing to the signal, the ratio $\frac{\omega^2}{\gamma^2 + \omega^2}$ varies from $1/2$ to 1, thus achieving a good damping of propagating waves.

To simplify the presentation we set $\xi_z = 1$ and $\varepsilon = \mu = 1$ for the remainder of the paper. Using the Fourier transform in time and algebraic manipulation in (10) we write the following time-dependent system of equations in the PML:

$$\partial_t E_y + \sigma_z(z)(E_y - P_y) = \partial_z H_x - \partial_x H_z \qquad (a)$$

$$\partial_t P_y + \gamma(P_y - E_y) = 0 \qquad (b)$$

$$\partial_t H_x + \sigma_z(z)(H_x - M_x) = \partial_z E_y \qquad (c)$$

$$\partial_t M_x + \gamma(M_x - H_x) = 0 \qquad (d)$$

$$\partial_t H_z - \sigma_z(z)H_z - (\gamma + \sigma_z(z))M_z = -\partial_x E_y \quad (e)$$

$$\partial_t M_z + (\gamma + \sigma_z(z))M_z + \sigma_z(z)H_z = 0. \qquad (f)$$

(13)

When $\sigma_z(z) = \gamma = 0$, (13) reduces to a symmetric (i.e., strongly well-posed) hyperbolic system for $\xi_z \geq 1$ (see Section 3 of [10], where the role of ξ_z is further elucidated), while when $\gamma = 0$ with $\sigma_z(z) \neq 0$, (13) reduces to the standard unsplit PML whose principal part is also a symmetric (i.e., strongly well-posed) hyperbolic system. System (13) will be used to derive the first-order energy estimate which generalizes (2)-(3) to the case $\gamma \neq 0$. It will be fruitful to rewrite it as a first-order symmetric hyperbolic system with a lower-order term for the field vector $\mathbf{U} = (E_y, P_y, H_x, M_x, H_z, M_z)^T$ as

$$\mathbf{U}_t + \mathbf{A}\mathbf{U}_z + \mathbf{B}\mathbf{U}_x + \mathbf{C}\mathbf{U} = 0. \tag{14}$$

Using (13) the 6×6 matrix $\mathbf{C}$ is identified as:

$$\mathbf{C} = \begin{pmatrix} \sigma_z(z) & -\sigma_z(z) & 0 & 0 & 0 & 0 \\ -\gamma & \gamma & 0 & 0 & 0 & 0 \\ 0 & 0 & \sigma_z(z) & -\sigma_z(z) & 0 & 0 \\ 0 & 0 & -\gamma & \gamma & 0 & 0 \\ 0 & 0 & 0 & 0 & -\sigma_z(z) & -(\sigma_z(z) + \gamma) \\ 0 & 0 & 0 & 0 & \sigma_z(z) & (\sigma_z(z) + \gamma) \end{pmatrix}. \tag{15}$$

To be completely defined, system (14) needs some initial conditions:

$$\mathbf{U}(t = 0) = \mathbf{U_0} \equiv (E_y^0, P_y^0, H_x^0, M_x^0, H_z^0, M_z^0)^T \tag{16}$$

For convenience, we introduce the space

$$X = (L^2(\mathbb{R}^2))^6$$

equipped with the norm:

$$\|\mathbf{U}\| = \left(\|E_y\|^2 + \|P_y\|^2 + \|H_x\|^2 + \|M_x\|^2 + \|H_z\|^2 + \|M_z\|^2 \right)^{1/2}$$

and with the associated scalar product denoted by $(.,.)_X$. We then have:

Theorem 2 *System (14)-(16) is well posed for any initial condition* $\mathbf{U_0} \in X$. *Furthermore, the solution satisfies the following estimate:*

$$\||\mathbf{U}(t)|\| \leq e^{\alpha t} \||\mathbf{U_0}|\| \tag{17}$$

where $\alpha = \|\sigma\|_{\infty} + \gamma$.

Proof: This is a consequence of the fact that system (14) is a zero-order perturbation of a symmetric hyperbolic system (thus strongly well posed) (see [18]). Then, multiplying (14) with $\mathbf{U}^T$, and using the symmetry of $\mathbf{A}$ and $\mathbf{B}$, one obtains:

$$\frac{d}{dt}\mathcal{E}_0(t) + \frac{1}{2}\int_{\mathbb{R}^2}[\partial_z(\mathbf{U}^T\mathbf{A}\mathbf{U}) + \partial_x(\mathbf{U}^T\mathbf{B}\mathbf{U})]dx + \int_{\mathbb{R}^2}(\mathbf{U}^T\mathbf{C}\mathbf{U})dx = 0 \tag{18}$$

where $\mathcal{E}_0$ denotes the standard zero-order field energy:

$$\mathcal{E}_0(t) = \frac{1}{2}\||\mathbf{U}(t)|\|^2$$

The middle integral in (18) vanishes by the Divergence Theorem leaving

$$\frac{d}{dt}\mathcal{E}_0(t) = -(\mathbf{C}\mathbf{U}, \mathbf{U})_X \tag{19}$$

The estimate follows easily from the Gronwall's lemma. ∎

Remark 1 *One can notice that, even though the problem is well-posed, estimate (17) does not prevent the solution to blow up exponentially when the time goes to infinity; in numerical calculations such a phenomenon is often described as an instability and is difficult to distinguish from a real ill-posedness of the equations. This is why in [12], a distinction is made between these two notions, and a system is characterized as stable if no exponential blow up of the solution is possible.*

4   Energy considerations for the new unsplit PML

Throughout this Section we will consider $\sigma_z(z) = \sigma$ to be a constant and, similarly, $\sigma_x(x) = \sigma$ when it arises. The generalization of this Section's results to the case of variable σ_x and σ_z will be given elsewhere.

First, we address the issue of long-time linear growth of the fields in the new PML from the point of view of [11]. When $\partial_x = 0$ and $\partial_z = 0$ are substituted in (14), the resulting system $\mathbf{U}_t = -\mathbf{C}\mathbf{U}$ decouples into three 2×2 systems. The first two such sub-systems, for (E_y, P_y) and (H_x, M_x), both exhibit the eigenvalues $(0, -(\sigma+\gamma))$, while the third, for the pair (H_z, M_z), exhibits the eigenvalues $(0, -\gamma)$. Hence, the linear growth in time, discussed in [11] for the unsplit PML with $\gamma = 0$, is absent from (13) when $\gamma \neq 0$, and the fields tend to a constant whose value depends on the initial conditions. At the same time the perfectly matched property is preserved by construction.

Next we consider the electromagnetic energy identity (19). If the right hand side of (19) is negative then we would have an estimate for the zero-order energy, i.e., $\mathcal{E}_0(t) \leq C$ where C is a time-independent constant. Unfortunately, the quadratic form under the integral, $\mathbf{U}^T\mathbf{C}\mathbf{U}$, is not strictly positive semi-definite since the symmetric part of $\mathbf{C}$ is indefinite. Therefore we have decided to attempt to determine whether the fields in the new PML are bounded in the long-time through the first- and second-order energy arguments given below.

4.1 A first-order energy decay result for the PML layer

We consider in this section problem (13) with $\sigma > 0$ and $\gamma > 0$. We introduce the first order energy:

$$
\begin{aligned}
2\mathcal{E}_1(t) &= \|(\partial_t + \gamma)H_z\|^2 + \|(\partial_t + \gamma + \sigma)E_y\|^2 + \|(\partial_t + \gamma)H_x\|^2 \\
&\quad + \sigma\left(2\gamma\|H_x\|^2 + \sigma\|H_x - M_x\|^2 + \sigma\|M_x\|^2\right)
\end{aligned}
\tag{20}
$$

Lemma 1 *The energy $\mathcal{E}_1$ of the solution of (13) satisfies the identity:*

$$
\frac{d}{dt}\mathcal{E}_1(t) = -2\sigma\left(\|\partial_t H_x\|^2 + \sigma\gamma\|H_x - M_x\|^2\right) \leq 0
\tag{21}
$$

which shows that it is decreasing in time.

Proof: the technique is very similar to the one used in [12]:

- we apply the operator $\partial_t + \gamma$ to equation (13)-(a) and multiply it by $(\partial_t + \gamma + \sigma)E_y$
- we apply the operator $\partial_t + \gamma + \sigma$ to equation (13)-(c) and multiply it by $(\partial_t + \gamma)H_x$
- we apply the operator $\partial_t + \gamma + \sigma$ to equation (13)-(e) and multiply it by $(\partial_t + \gamma)H_z$

and we add the three identities. Using that σ (resp. γ) is constant, one can commute ∂_z and σ (resp. ∂_z and γ) so that the terms containing the space derivatives vanish. It remains

$$
A_1 + A_2 + A_3 = 0
$$

with

$$
A_1 = ((\partial_t + (\gamma + \sigma))(\partial_t - \sigma)H_z, (\partial_t + \gamma)H_z) - ((\gamma + \sigma)(\partial_t + (\gamma + \sigma))M_z, (\partial_t + \gamma)H_z)
$$

$$
A_2 = (\partial_t(\partial_t + \gamma)E_y, (\partial_t + (\gamma + \sigma))E_y) + (\sigma(\partial_t + \gamma)(E_y - P_y), (\partial_t + (\gamma + \sigma))E_y)
$$

$$
A_3 = ((\partial_t + (\gamma + \sigma))\partial_t H_x + \sigma(\partial_t + \gamma + \sigma)(H_x - M_x), (\partial_t + \gamma)H_x)
$$

It is easy to rewrite the first term, using (13)-(f) as

$$
A_1 = ((\partial_t + (\gamma + \sigma))(\partial_t - \sigma)H_z, (\partial_t + \gamma)H_z) + ((\gamma + \sigma)\sigma H_z, (\partial_t + \gamma)H_z) = \frac{1}{2}\frac{d}{dt}\|(\partial_t + \gamma)H_z\|^2
$$

The second term can be rewritten using (13)-(b) as

$$
A_2 = (\partial_t(\partial_t + \gamma)E_y + \sigma(\partial_t + \gamma) - \sigma\gamma E_y, (\partial_t + (\gamma + \sigma))E_y) = \frac{1}{2}\frac{d}{dt}\|(\partial_t + \gamma + \sigma)E_y\|^2
$$

For the third term, we have to work a little more and we first decompose it in the following way:

$$
A_3 = (\partial_t + \gamma)\partial_t H_x + \sigma\partial_t H_x + \sigma(\partial_t + \gamma + \sigma)H_x - \sigma(\partial_t + \gamma)M_x - \sigma M_x, (\partial_t + \gamma)H_x)
$$

Using (13)-(d), this can be rewritten as

$$
\begin{aligned}
A_3 &= ((\partial_t + \gamma)\partial_t H_x, (\partial_t + \gamma)H_x) + \sigma(2\partial_t H_x + \sigma(H_x - M_x), (\partial_t + \gamma)H_x) \\
&= \frac{1}{2}\frac{d}{dt}\|(\partial_t + \gamma)H_x\|^2 + 2\sigma\|\partial_t H_x\|^2 + 2\sigma\gamma\frac{1}{2}\frac{d}{dt}\|H_x\|^2 \\
&\quad + \sigma^2(H_x - M_x, \partial_t H_x) + \sigma^2\gamma(H_x - M_x, H_x)
\end{aligned}
$$

7

To conclude, we remark first, (again using (13)-(d)):

$$(H_x - M_x, \partial_t H_x) = (\partial_t(H_x - M_x), H_x - M_x) + (\partial_t M_x, H_x - M_x) = \frac{1}{2}\frac{d}{dt}\|H_x - M_x\|^2 + \gamma\|H_x - M_x\|^2$$

and in the same way:

$$
\begin{aligned}
\gamma(H_x - M_x, H_x) &= \gamma\|H_x - M_x\|^2 + \gamma(H_x - M_x, M_x) = \gamma\|H_x - M_x\|^2 + (\partial_t M_x, M_x)\\
&= \gamma\|H_x - M_x\|^2 + \frac{1}{2}\frac{d}{dt}\|M_x\|^2
\end{aligned}
$$

Therefore

$$
\begin{aligned}
A_3 &= \frac{1}{2}\frac{d}{dt}\left(\|(\partial_t + \gamma)H_x\|^2 + 2\sigma\gamma\|H_x\|^2 + \sigma^2\|H_x - M_x\|^2 + \sigma^2\|M_x\|^2\right)\\
&\quad + 2\sigma\|\partial_t H_x\|^2 + 2\sigma^2\gamma\|H_x - M_x\|^2
\end{aligned}
$$

∎

Theorem 3 *The solution of (13) satisfies the following estimate,*

$$\|H_x(t)\| + \|H_z(t)\| \le \||\mathbf{U_0}\|| + \frac{\mathcal{E}_1^{1/2}(0)}{\gamma}$$

$$\|E_y(t)\| \le \||\mathbf{U_0}\|| + \frac{\mathcal{E}_1^{1/2}(0)}{\sigma + \gamma}$$

(22)

Proof: these estimates are a consequence of lemma 1 and of the following technical lemma. ∎

Lemma 2 *Let G be a function defined in $L^\infty(0, \infty, L^2(\mathbb{R}^2))$, and $\mathcal{G}$ its norm:*

$$\mathcal{G} = \sup_{t \ge 0}\|G(t)\|$$

Let H be related to G through the following differential equation

$$\partial_t H + \gamma H = G, \quad H(0) = H_0$$

then it satisfies the following estimate

$$\|H(t)\| \le C_\gamma, \quad \forall t > 0$$

where $C_\gamma = \|H_0\| + \mathcal{G}/\gamma$.

Proof : The solution of the ordinary differential equation is determined by:

$$H(x, t) = H_0(x)e^{-\gamma t} + \int_0^t G(x, s)e^{-\gamma(t-s)}ds$$

so that

$$\|H(t)\| \le \|H_0\|e^{-\gamma t} + \left\|\int_0^t G(x, s)e^{-\gamma(t-s)}ds\right\|$$

Using the identity:

$$\left(\int_0^t G(x, s)e^{-\gamma(t-s)}ds\right)^2 = \left(\int_0^t G(x, s)e^{-\gamma(t-s)}ds\right)\left(\int_0^t G(x, u)e^{-\gamma(t-u)}du\right)$$

8

it is then easy to show that

$$\left\|\int_0^t G(x,s)e^{-\gamma(t-s)}ds\right\|^2 \leq \int_0^t \int_0^t e^{-\gamma(t-s)-\gamma(t-u)}\|G(s)\|\,\|G(u)\|\,dsdu$$

$$\leq \mathcal{G}^2\left(\frac{1-e^{-\gamma t}}{\gamma}\right)^2 \leq \frac{\mathcal{G}^2}{\gamma^2}$$

which allows to conclude. ∎

As a consequence of Theorem 3, it is easy to see, using the equations (13) at the initial time $t=0$ in order to rewrite the initial first-order energy $\mathcal{E}_1(0)$ with respect to the initial conditions, that if $\mathbf{U_0} \in X$ and additionally $\left(\vec{\text{rot}}\, E_y^0, \text{rot}\,\vec{H}^0\right) \in (L^2(\mathbb{R}^2))^2 \times L^2(\mathbb{R}^2)$, the solution of (13) satisfies the estimate: there exists a constant $C > 0$ independent of t such that

$$\|H_x(t)\| + \|H_z(t)\| \leq C\left((1+\frac{1}{\gamma})\,|\|\mathbf{U_0}\|| + \frac{1}{\gamma}\left\|\vec{\text{rot}}\, E_y^0\right\| + \frac{1}{\gamma}\left\|\text{rot}\,\vec{H}^0\right\|\right)$$

$$\|E_y(t)\| \leq C\left((1+\frac{1}{\sigma+\gamma})\,|\|\mathbf{U_0}\|| + \frac{1}{\sigma+\gamma}\left\|\vec{\text{rot}}\, E_y^0\right\| + \frac{1}{\sigma+\gamma}\left\|\text{rot}\,\vec{H}^0\right\|\right)$$

(23)

4.2   A second-order energy decay result for the PML corner

For the new unsplit PML in a corner, where the $\hat{x}-$directed layer overlaps the $\hat{z}-$directed layer, and for $\sigma_x(x) = \sigma_z(z) = \sigma$ constant, the governing equations are (see the Appendix of [10], and do some differentiation of integrals using Leibnitz's Rule):

$$\partial_t E_y + 2\sigma E_y + \sigma^2(1-\tfrac{2\gamma}{\sigma})P - \sigma^2\gamma Q = \partial_z H_x - \partial_x H_z \quad (a)$$

$$\partial_t H_x = \partial_z E_y \qquad\qquad\qquad (b)$$

$$\partial_t H_z = -\partial_x E_y \qquad\qquad\qquad (c) \qquad (24)$$

$$(\partial_t + \gamma)P = E_y \qquad\qquad\qquad (d)$$

$$(\partial_t + \gamma)Q = P \qquad\qquad\qquad (e).$$

In contrast to the case $\gamma = 0$, we have not been able to derive a zero-order energy decay result for (24). We proceed with an identity satisfied by a second-order energy, defined as:

$$2\mathcal{E}_2(t) = \left\|(\partial_t + \gamma)^2 H_z\right\|^2 + \left\|(\partial_t + \gamma)^2 H_x\right\|^2 + \left\|(\partial_t + \gamma)^2 E_y\right\|^2$$

$$+\sigma^2\left(\|\partial_t E_y\|^2 + \|\gamma E_y\|^2\right)$$

(25)

Lemma 3 *The energy $\mathcal{E}_2$ of the solution of (24) satisfies the identity:*

$$\frac{d}{dt}\mathcal{E}_2(t) = -2\sigma\left(\|\partial_t(\partial_t + \gamma)E_y\|^2 + \sigma\gamma\|\partial_t E_y\|^2\right) \leq 0$$

(26)

which shows that it is decreasing in time.

Proof: The technique is very similar to the one used in Lemma 1:

- we apply the operator $(\partial_t + \gamma)^2$ to equation (24)-(a) and multiply it by $(\partial_t + \gamma)^2 E_y$

- we apply the operator $(\partial_t + \gamma)^2$ to equation (24)-(b) and multiply it by $(\partial_t + \gamma)^2 H_x$

9

- we apply the operator $(\partial_t + \gamma)^2$ to equation (24)-(c) and multiply it by $(\partial_t + \gamma)^2 H_z$

Similar manipulations lead to the stated result. ■

Theorem 4 *The solution of (24) satisfies the following estimate:* $\exists C_\gamma > 0$ *independent of t such that*

$$\|H_x(t)\| + \|H_z(t)\| + \|E_y(t)\| \leq C_\gamma \qquad (27)$$

where C_γ depends on the initial conditions and on γ as $1/\gamma^2$ for small γ.

Proof: Again, these estimates are a consequence of Lemma 3 and of the technical Lemma 2. ■

One can notice that the estimate (27) does not reduce to (5) as $\gamma \to 0$. Also, the attempt to estimate a zero-order energy did not lead us to an estimate like (17). In our numerical simulations, we do not consider a problem where the computational domain requires a corner layer for the PML implementation.

5   Numerical Experiments

A two-dimensional simulation of an electric line source exciting a parallel plate waveguide with perfectly conducting walls was performed as a validation of the energy estimates given in Section 4. The problem space is illustrated in Figure 1. The space was discretized via a two-dimensional Yee lattice with uniform grid spacing $\Delta x = \Delta z = 1mm$. The center of the lattice was excited by a $\hat{y}-$directed point-current source, thus launching a TM_y wave. The source had a time signature given by either

$$J_y(t) = e^{-\frac{(t-t_o)^2}{t_w^2}} \sin 2\pi f_c t, \qquad (28)$$

or

$$J_y(t) = -2\frac{t}{t_w}e^{-\frac{(t-t_o)^2}{t_w^2}} \sin 2\pi f_c t, \qquad (29)$$

where $t_w = 3.183 \times 10^{-10}$ sec, $t_o = 4t_w$ and $f_c = 3 \times 10^9$ Hz. The normal-to$-\hat{z}$ boundaries were terminated with a 10 cell thick PML, itself terminated with a perfect electric conductor boundary condition on the tangential electric field E_y. The conductivity of the PML was scaled using polynomial scaling with $m = 4$ and $\sigma_{max} = 10.61$ S/m. The simulations with source (28) were performed with a time step of $\Delta t = 1.9065 \times 10^{-12}$ sec, while those with (29) were performed with a time step of $\Delta t = 2.35 \times 10^{-12}$ sec or $\Delta t = 1.175 \times 10^{-12}$ sec. Three values of γ are considered, $\gamma = 0$, 0.08, 0.16.

Initially, the simulation was performed using the standard unsplit PML ($\gamma = 0$) with source (28); it was run for $100,000$ timesteps, and the fields were sampled at spatial index $(31, 59)$ and $(31, 31)$. Figure 2-(a) illustrates the late-time response of the axial Magnetic field, H_z, in the PML; it is observed that it exhibits a linear growth in time while the remaining field components tend to zero in full accordance with the discussion following Eq. (2)-(3).

Next, this simulation was repeated with $\gamma = 0.08$. The late-time fields are shown in Figure 2-(b). Now, all field components remain bounded by a time-independent constant in full agreement with our energy considerations in Section 4.

To test whether the zero-frequency content introduced by the sharp turn-on of the source is responsible for the late-time DC offset exhibited by the computed fields when $\gamma > 0$ we repeated the two previously described simulations with source (29). The results in Figure 3-(a) show that the late-time linear growth of the axial magnetic field in the PML is independent of the source's DC spectral content, again verifying the discussion following Equations (2)-(3). Figure 3-(b) shows that when $\gamma = 0.08$ only the axial magnetic field tends to a constant while the other field components decay to zero. Again, this is in agreement with our energy considerations given in Section 4. For this set of simulations we also graphed the axial magnetic field inside the computational domain; Figure 4 shows that the axial field decays to zero in the late time for
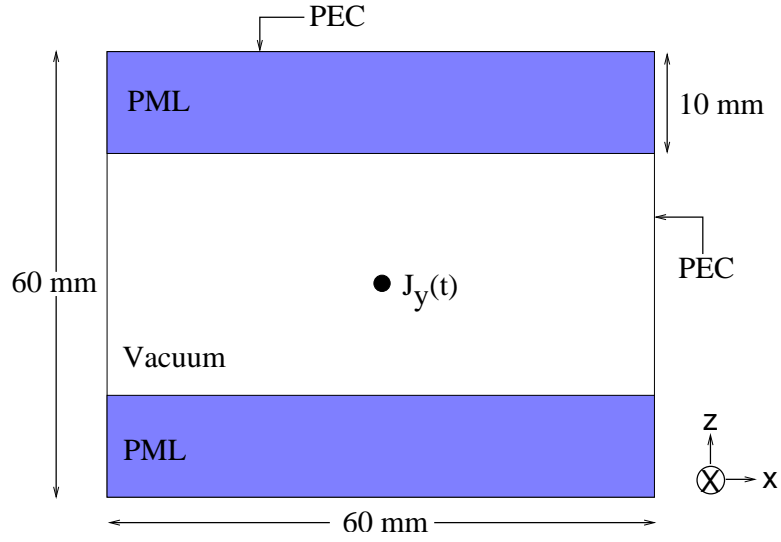
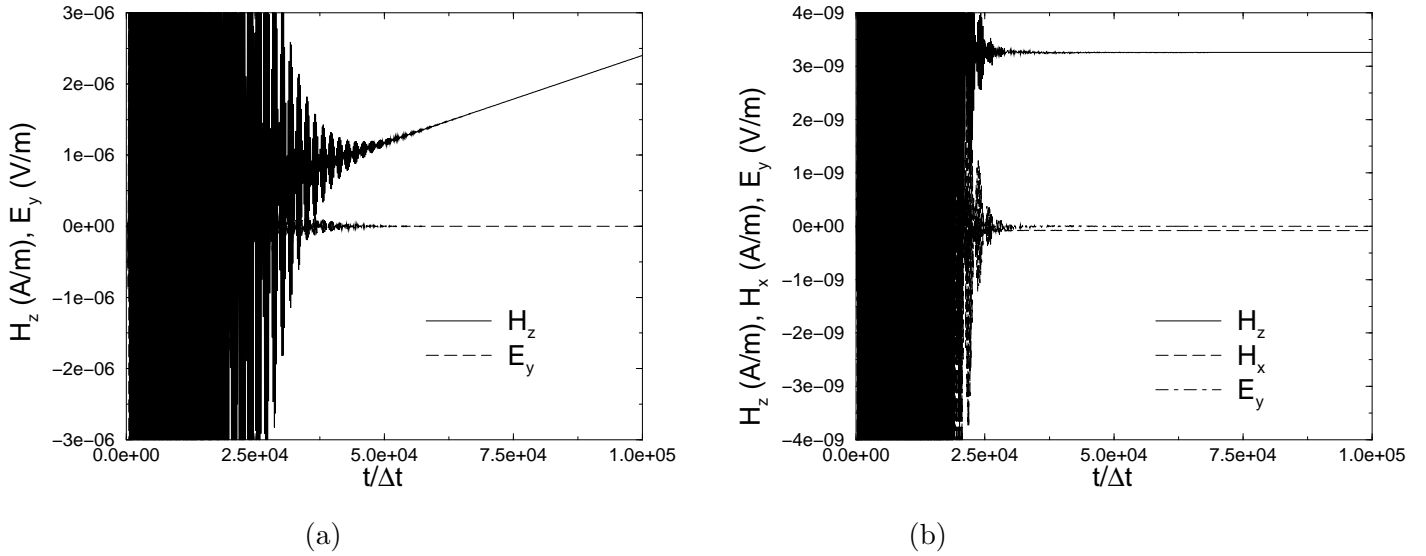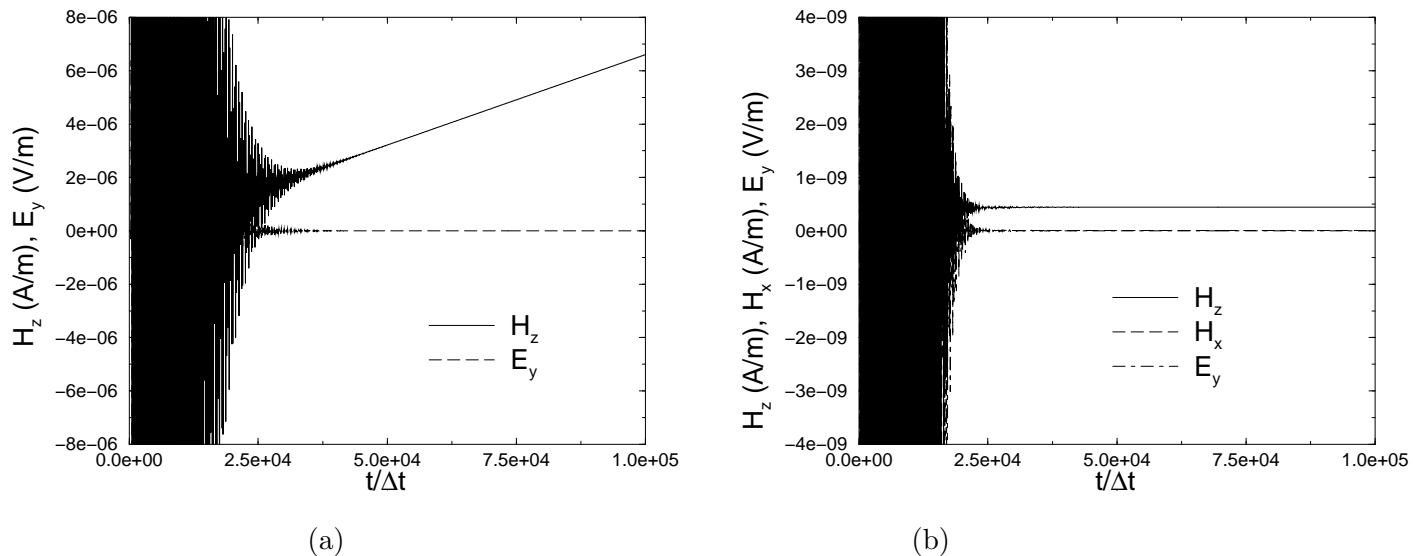Figure 1: Geometry of the numerical experiments.

(a)

(b)

Figure 2: For source (28): a) The late-time linear growth of the axial PML field, $H_z(31, 59, t)$. The $H_x(31, 59, t)$ field behaves exactly like the graphed electric field $E_y(31, 59, t)$. This case, $\gamma = 0$, represents the standard unsplit PML. b) $\gamma = 0.08$; the late-time linear growth of H_z has been removed.
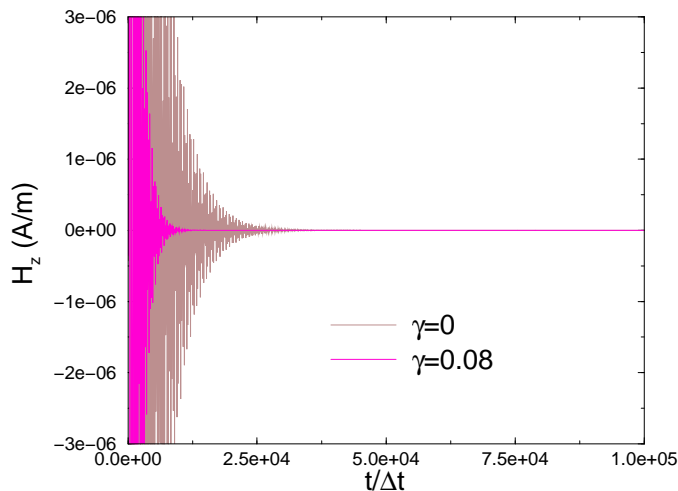
(a)   (b)

Figure 3: For source (29): a) The late-time linear growth of the axial PML field, $H_z(31, 59, t)$. The $H_x(31, 59, t)$ field behaves exactly like the graphed electric field $E_y(31, 59, t)$. This case, $\gamma = 0$, represents the standard unsplit PML. b) $\gamma = 0.08$; the late-time linear growth of H_z has been removed.

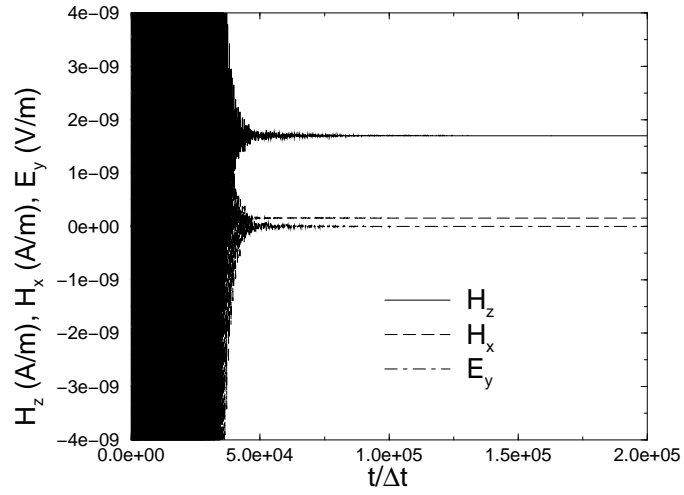Figure 4: The axial magnetic field, $H_z(31, 31, t)$, inside the computational domain for source (29).

Figure 5: Same as Figure 3-(b) but with $\Delta t/2$ timestep.
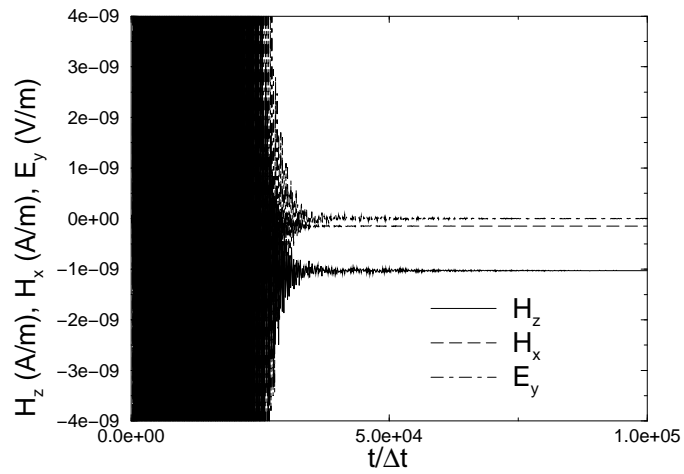
Figure 6: Same as Figure 5 but with $\gamma = 0.16$.

13

$\gamma \geq 0$, hence the linear growth indicated above for $\gamma = 0$ is restricted to the PML layer (at least for the time interval considered herein $\approx 7.4 \times 10^4$ source durations). Figure 5 shows the effect of a reduction in the timestep with $\gamma = 0.08$. Again, the fields in the PML remain bounded by a time-independent constant. Finally, Figure 6 verifies the dependence of the field estimates on γ since in this case doubling this parameter reduces the long-time constant value of the fields H_z and H_x (while leaving the value of E_y largely unaffected) in accordance to (22); these long-time values should be compared to those shown in Figure 5. As it is evident from all the Figures, the long-time value of E_y is not sensitive to the variation in γ since $\sigma \gg \gamma$ (see second relation in (22)).

6   Conclusion

With analysis and numerical experiments we explained how the Complex Frequency Shifted scaling function (9) eliminates the long-time linear growth, identified in [11], of the fields in the unsplit PML while maintaining the perfectly matched property of the equations. Also, we showed via energy arguments that all the fields in the new unsplit PML are bounded by time-independent constants. The present work, together with the numerical results on the absorption properties of the CFS scaling function for elongated domains [15], indicate that the resulting unsplit PML is the most suitable for problems requiring long-time integration of the time-domain Maxwell equations. Also, it is suitable for problems with significant low-frequency and/or evanescent-wave content [17].

Acknowledgments

References

[1] J. P. Bérenger, "A Perfectly Matched Layer for the Absorption of Electromagnetic Waves," *J. Comput. Physics*, vol. 114, pp. 185-200, 1994.

[2] L. Zhao and A. C. Cangellaris, "GT-PML: Generalized Theory of Perfectly Matched Layers and its Application to the Reflectionless Truncation of Finite-Difference Time-Domain Grids", *IEEE Trans. Microwave Theory Tech.*, vol. 44, pp. 2555-2563, 1996.

[3] S. D. Gedney, "An Anisotropic Perfectly Matched Layer-Absorbing Medium for the Truncation of FDTD Lattices," *IEEE Trans. Antennas Propagat.*, vol. 44, pp. 1630-1639, 1996.

[4] F. Q. Hu, "A Stable, Perfectly Matched Layer for Linearized Euler Equations in Unsplit Physical Variables", *Journal of Computational Physics*, vol. 173, no. 2, pp. 455-480, 2001.

[5] J. S. Hesthaven, "On the Analysis and Construction of Perfectly Matched Layers for the Linearized Euler Equations", *Journal of Computational Physics*, vol. 142, pp. 129–147, 1998.

[6] F. Collino and C. Tsogka, "Application of the PML Absorbing Layer Model to the Linear Elastodynamic Problem in Anisotropic Heterogeneous Media", *Geophysics*, vol. 66, no. 1, pp. 294-1307, 2001.

[7] I. M. Navon, B. Neta and M. Y. Hussaini, "A perfectly matched layer formulation for the nonlinear shallow water equation models: The split equation approach", *Monthly Weather Review*, to appear, 2001.

[8] S. Abarbanel and D. Gottlieb, "A Mathematical Analysis of the PML Method", *J. Comput. Physics*, vol. 134, pp. 357-363, 1997.

[9] P. G. Petropoulos, L. Zhao and A. C. Cangellaris, "A Reflectionless Sponge Layer Absorbing Boundary Condition for the Solution of Maxwell's Equations with High-Order Staggered Finite Difference Schemes", *J. Computational Physics*, vol. 139, pp. 184-208, 1998.

[10] P. G. Petropoulos, "Reflectionless Sponge Layers as Absorbing Boundary Conditions for the Numerical Solution of Maxwell's Equations in Rectangular, Cylindrical and Spherical Coordinates", *SIAM J. App. Math.*, vol. 60, no. 3, pp. 1037-1058, 2000.

[11] S. Abarbanel, D. Gottlieb and J. S. Hesthaven, "Long Time Behavior of the Perfectly Matched Layer Equations in Computational Electromagnetics," *Journal of Scientific Computing*, vol. 17, no. 1-4, pp. 405-422, 2002.

[12] E. Bécache and P. Joly, "On the analysis of Bérenger's Perfectly Matched Layers for Maxwell's equations," *Mathematical Modelling and Numerical Analysis*, vol. 36, no. 1, pp. 87-119, 2002.

[13] M. Kuzuoglu and R. Mittra, "Frequency Dependence of the Constitutive Parameters of Causal Perfectly Matched Anisotropic Absorbers," *IEEE Microwave and Guided Wave Letters*, vol. 6, pp. 447-449, 1996.

[14] S. D. Gedney, "The Perfectly Matched Layer Absorbing Medium," *Advances in Computational Electrodynamics: The Finite-Difference Time-Domain Method*, A. Taflove (Editor), Artech House, Boston, MA, 1998, pp. 263-340.

[15] J. A. Roden and S. D. Gedney, "Convolutional PML (CPML): An Efficient FDTD Implementation of the CFS-PML for Arbitrary Media," *Microw. Opt. Tech. Letters*, vol. 27, pp. 334-339, 2000.

[16] W. H. Yu, R. Mittra R and S. Chakravarty, "Stability characteristics of absorbing boundary conditions in microwave circuit simulations," *IEEE Trans. Antennas Propagat.*, vol. 49, pp. 1347-1349, 2001.

[17] J. P. Bérenger, "Application of the CFSPML to the absorption of evanescent waves in waveguides," *IEEE Microwave and Guided Wave Letters*, vol. 12, pp. 218-220, 2002.

[18] H- O. Kreiss and J. Lorenz, *Initial-Boundary Value Problems and the Navier-Stokes Equations*, Academic Press, 1989.

[19] J. De Moerloose and D. De Zutter, "Poynting's theorem for the finite-difference - time-domain method," *Microw. Opt. Tech. Letters*, vol. 8, no. 5, pp. 257-260, 1995.